Measurement of the refractive index of highly turbid media

W. R. Calhoun, H. Maeta, A. Combs, L. M Bali, and S. Bali*

Department of Physics, Miami University, Oxford, Ohio 45056-1866, USA
**Corresponding author: balis@muohio.edu*

Received January 6, 2010; accepted February 16, 2010;
posted March 19, 2010 (Doc. ID 122190); published April 15, 2010

We demonstrate a first simultaneous measurement of the real and imaginary parts of the refractive index of a *highly* turbid medium by observing the real-time reflectance profile of a divergent laser beam made incident on the surface of the turbid medium. We find that the reflectance data are well described by Fresnel theory that correctly includes the effect on total internal reflection of angle-dependent penetration into the turbid medium.

OCIS codes: 120.1840, 120.4640, 120.5710, 120.5820, 280.1415, 290.7050.

The term "turbid media" refers to disordered, or random, media such as colloidal suspensions that generate extensive multiple scattering of the incident light. Quantitatively, turbidity is described by the attenuation coefficient (α), which measures the loss of directed radiation per unit length through the sample due to scattering and/or absorption; i.e., the intensity $I(z)$ of a light beam propagating in the z direction through the medium can be written as $I(z) = I_0 \exp(-\alpha z)$, where I_0 is the intensity at $z=0$. For example, the value of α for milk in the visible and near-IR frequencies ranges between 40 and 125 cm^{-1} depending on fat content. We consider media with $\alpha > 200\ \text{cm}^{-1}$ as highly turbid—examples include biotissue [1] and crude petroleum [2].

The measurement of the complex refractive index of a turbid medium has received considerable attention [1–6]. The imaginary component n_i of the refractive index stems from scattering and/or absorption in the medium; hence its measurement involves propagation through the medium. On the other hand, the real part n_r arises from the bending of an incident light ray at the surface of the medium and is typically determined by a measurement of the critical angle for total internal reflection (TIR). A real-time measurement of the complex refractive index, which would permit instantaneous monitoring of changes in the medium, necessarily means a simultaneous measurement of both the real and the imaginary parts.

The question arises, is it possible to simultaneously measure, in real-time, the real and imaginary parts of the refractive index for highly turbid media? And, if so, can the data be explained accurately with a valid theoretical model in order to extract meaningfully accurate values for the refractive index and attenuation coefficient? The answer is not straightforward, because, as is well known, the critical angle is not a well-defined concept for highly turbid media [5,6]. For this reason previous methods for measuring the refractive index that relied on determining the critical angle [1,4] fail for highly turbid media.

Reyes-Coronado *et al.* [5] cited "persistent inconsistencies" [4] in the use of traditional Fresnel relations to model the reflectance from a turbid medium and instead demonstrated a real-time measurement of the complex refractive index by measuring the *transmittance* of a light beam through a thin prism filled with a colloidal suspension of polystyrene spheres, while at the same time determining the angle by which the light beam refracts through the prism. However, this transmission-based method was demonstrated in [5] only for moderately turbid colloidal suspensions, with $\alpha < 40\ \text{cm}^{-1}$.

Niskanen *et al.* [6] worked with far more turbid samples ($\alpha \leqslant 800\ \text{cm}^{-1}$) by using both transmission and reflection measurements. They designed a spectrophotometer that measures n_i by transmission at normal incidence through a thin turbid sample and subsequently measures n_r by reflection from the sample surface as the incident angle is varied. However, this is not a simultaneous measurement of the instantaneous n_r and n_i. More important, the authors in [6] employ an empirical model for which they offer no justification other than that it has been "observed to be useful" in making their fits agree with the data whenever their measurement "departs strongly" from traditional Fresnel theory.

In this Letter we demonstrate a first simultaneous measurement of the real and imaginary parts of the refractive index of highly turbid media. We achieve this by observing the real-time reflectance profile of a divergent laser beam incident on the surface of the turbid medium. This geometry, particularly in the context of a collimated beam, has been considered before [4,6]. However, the Fresnel theory for TIR from a turbid medium has not been correctly applied to date, leading to significant discrepancy between the theory and data. We resolve this discrepancy by incorporating into the Fresnel theory the effect on TIR of angle-dependent penetration by the divergent beam into the turbid medium. We employ no empirically defined fitting parameters in our model. The attenuation coefficient α for the most turbid samples used in the work presented here ranges up to 1200 cm^{-1}, i.e., a factor 30 higher than that used in previous simultaneous measurements of the real and imaginary refractive indices by other researchers. Our method should apply to samples with much higher turbidity. Furthermore, owing to the elimination of mechanical noise (no moving parts), our method is 1 order of

0146-9592/10/081224-3/$15.00

magnitude higher, if not more, in sensitivity to changes in n_r and/or n_i than previous methods [5,6]. Though the work here is presented for a single wavelength, it should be straightforward to extend the method to a multiwavelength source.

The basic principle of TIR-based refractive index measurement is depicted in Fig. 1(a). A sample of refractive index n_{sample} is placed on top of a glass prism of known refractive index n_{prism} ($>n_{\text{sample}}$). The sample refractive index is written in terms of a real part n_r and an imaginary part n_i as $n_{\text{sample}}=n_r+in_i$. The attenuation coefficient α is related to n_i as $\alpha=2n_i\omega/c$, where ω is the laser frequency and c is the speed of light [7]. If the sample is transparent ($\alpha=0$), we find on varying the incident angle θ_i that we encounter a critical angle θ_c at which the angle of refraction θ_r becomes 90°. When $\theta_i>\theta_c$, TIR at the prism–sample interface is observed. Thus, for transparent samples, one may simply apply Snell's law to obtain $n_{\text{sample}}=n_{\text{prism}}\sin\theta_c$. In Fig. 1(b) the curve marked "$\alpha=0$" shows a theoretical reflectance profile $I_r/I_i(\theta_i)$ for a transparent medium in accordance with the usual Fresnel relation, $I_r/I_i(\theta_i)=[\tan^2(\theta_i-\theta_r)]/[\tan^2(\theta_i+\theta_r)]$, where we assume the incident beam to be polarized parallel to the plane of incidence [7]. The vertical dotted line in Fig. 1(b) marks the sharp transition between the TIR and non-TIR regions, thus locating the critical angle θ_c and hence n_{sample}. Recently, we demonstrated real-time refractometry at the one part-per-million level in transparent samples [8].

On the other hand, for highly turbid media the transition between the TIR and non-TIR regions of the reflectance profile is significantly more gradual, as depicted in Fig. 1(b) by the two curves marked "$\alpha=200$" and "$\alpha=1000$." The traditional approach to turbid media is to simply allow n_{sample} to be complex in the Fresnel equation written above for $I_r/I_i(\theta_i)$, yielding [4]

$$\frac{I_r}{I_i}=\frac{M+P^2\cos^2\theta_i-\sqrt{2}\cos\theta_i(M+\sin^2\theta_i)\sqrt{M+L}}{M+P^2\cos^2\theta_i+\sqrt{2}\cos\theta_i(M+\sin^2\theta_i)\sqrt{M+L}}, \tag{1}$$

where we have used $P=(n_r^2+n_i^2)/n_{\text{prism}}^2$, $L=[(n_r^2-n_i^2)/n_{\text{prism}}^2]-\sin^2\theta_i$, and $M=\sqrt{P^2-2L\sin^2\theta_i-\sin^4\theta_i}$. The $\alpha\neq 0$ reflectance plots in Fig. 1 have been drawn by using Eq. (1) for two turbid media of different yet constant values for n_i (and therefore α), and the same n_r value as the transparent medium. These plots emphasize that in order to simultaneously determine the real and imaginary components of the refractive index of a turbid medium, it is important to make detailed reflectance measurements over a range of angles around the TIR–non-TIR transition, not just at the transition itself. For angles just below the TIR–non-TIR transition, the overlap in the non-TIR region for the three media suggests that the reflectance there is dominated by n_r. On the other hand, for angles just above the TIR–non-TIR transition, it is n_i that dominates. This is because in TIR the ray

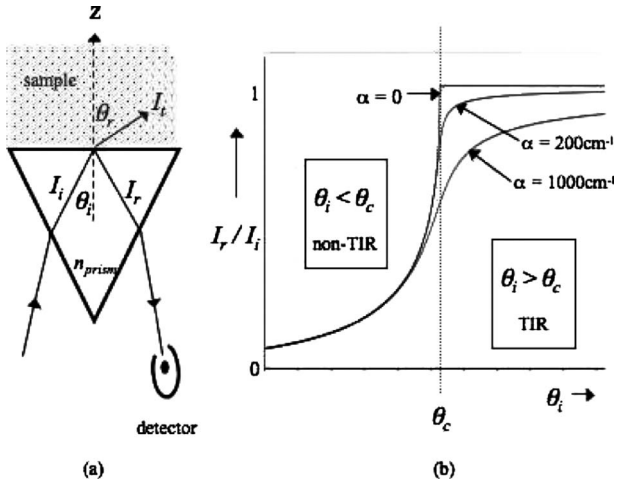

Fig. 1. (a) Prism–sample interface. (b) Plots of $I_r/I_i(\theta_i)$ from Eq. (1) for a transparent medium ($\alpha=0$) and two highly turbid media, all with the same n_r.

actually penetrates into the sample, so the reflected ray does not originate from the point at which the incident ray strikes the sample face, emerging instead from a laterally displaced point (the Goos–Hanchen shift [9]). During this penetration the loss incurred due to scattering in the turbid medium causes an attenuation of $I_r/I_i(\theta_i)$ in the vicinity of the TIR–non-TIR transition. Our data below show that Eq. (1), as used above, succeeds qualitatively but fails quantitatively in predicting this attenuation.

The experimental setup for real-time measurement of the reflectance profile is based on Fig. 1(a) and is essentially the same as already described in [8]. The sample (less than 0.1 ml is sufficient) is placed on top of a prism (equilateral, side 2.5 cm, F2 glass; $n_{\text{prism}}=1.614805$ at 660 nm, calculated by using a dispersion formula supplied by the manufacturer). The light source is a diode laser (660 nm) pigtailed to a single-mode fiber (NA 0.12). The fiber outputs a divergent beam with a Gaussian profile, which is made incident on the prism. The beam is reflected from the prism–sample interface onto a 1D pixel array (1024 pixels, pixel diameter 14 μm). Where TIR occurs the pixels are brightly illuminated, otherwise not, leading to an edge between dark and light regions of the reflected beam profile. For a transparent sample this edge is sharply defined, but for turbid samples it is manifested as a gradual reduction of intensity spread over many pixels. The profile $I_r/I_i(\theta_i)$ is obtained in three steps [8] by using a LabVIEW program: we first associate a unique angle of incidence θ_i with the center of each pixel by calibrating our refractive index measurements to those of a state-of-the-art commercial refractometer using two separate transparent calibration fluids [8]. Next we obtain $I_i(\theta_i)$ by measuring the reflectance curve for air (no sample present), for which TIR occurs over the entire range of incident angles subtended by the laser, thus reproducing the Gaussian laser beam on the pixel array. Finally we place the sample on the prism, measure $I_r(\theta_i)$, and compute the ratio $I_r(\theta_i)/I_i(\theta_i)$.

In Fig. 2 we show measured reflectance profiles for two highly turbid media formed by milk–cream mixtures. The values of n_r and n_i are determined from a least-χ^2 fit [dark gray curves (i) and (iii) in Fig. 2] by using Eq. (1), modified to include the effect of angle-dependent penetration by the divergent incident beam into the turbid medium. The assumption, used earlier in plotting the turbid reflectance profiles in Fig. 1(b), is that n_i (and α) in Eq. (1) is constant, which is not valid. Note that the penetration depth, defined as the depth at which the intensity of the evanescent wave drops to $1/e$ of its initial value, varies with θ_i, going from a few nanometers at incident angles far above the TIR–non-TIR transition to a few hundred nanometers at incident angles in the vicinity of the transition. The attenuation coefficient α is just the reciprocal of this penetration depth, thus ascribing an angular dependence to α, and therefore also to n_i. From the Fresnel theory for refraction into a turbid medium [7] we find that this new angular-dependent $n_i(\theta)$ can be written in terms of the original n_i (defined at normal incidence) as

$$n_i(\theta) = n_i(4\pi n_{\text{prism}}\sqrt{(M-L)/2})^{-1}. \quad (2)$$

The dark-curve theoretical fits in Fig. 2 are obtained by substituting $n_i(\theta)$ for n_i into Eq. (1), not the constant n_i. Note that no extraneous empirically defined fitting parameters were introduced. By contrast, the lighter gray curves (ii) and (iv) in Fig. 2 are plotted for the same n_r values as the dark curve fits for (i) and (iii), respectively, but erroneously use a constant n_i in Eq. (1). To explain the strong discrepancy between the light gray curve fits and the data, previous workers [4,6] speculated that their reflectance data were contaminated by light diffusely scattered from the turbid medium into the detector. Building on an idea proposed in [4], Niskanen *et al.* [6] proposed a modified reflectance R^+ defined as $R^+ = R + \phi R^m(1-R)$, where R is the reflectance I_r/I_i in Eq. (1), while ϕ and m represent free parameters, arbitrarily introduced to describe the detected diffuse scattering. No scientific justification is given for their introduction, nor of the values they attain ($m = 1.5$ in [6]) during the fitting. The empirical model in [4,6] predicts unrealistically large detected diffuse scattering (several percent of I_i).

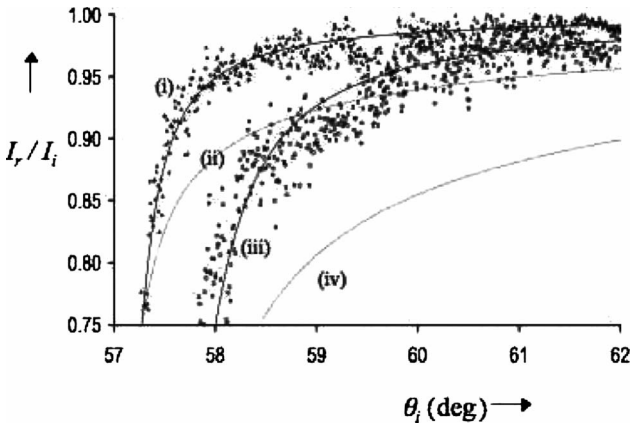

Fig. 2. $I_r/I_i(\theta_i)$ measured at 660 nm for milk–cream mixtures with (i) 10% fat and (iii) 33% fat. The dark curves (i) and (iii) are least-χ^2 fits using Eqs. (1) and (2), and incorporate angle-dependent penetration into the medium. The lighter gray curves (ii) and (iv) erroneously do not (see text). We obtain (i) $n_r = 1.35692$, $n_i = 0.00277$ ($\alpha = 527.60\ \text{cm}^{-1}$), and (iii) $n_r = 1.36541$, $n_i = 0.00618$ ($\alpha = 1177.0\ \text{cm}^{-1}$).

We compared our n_r measurements with a state-of-the-art commercial refractometer for three transparent ($n_i = 0$) water–glycerin mixtures (not the same as the calibration fluids mentioned above), and found perfect agreement to 1 part in 10^5, which is the sensitivity limit for the commercial device. For turbid media the commercial device measures n_r by defining an *ad hoc* "effective critical angle" as the point of maximum change of slope in the $I_r/I_i(\theta_i)$ curve. This fails even on a qualitative level: as shown in Fig. 1(b), even though the three media depicted are assigned the same n_r value, the point of maximum change of slope of $I_r/I_i(\theta_i)$ progresses rightward as turbidity increases. There are no reliable references with which to compare our n_i measurements: previous work at this turbidity is based on non-rigorously-justified empirical theory [6], or is performed after heavy dilution followed by extrapolation [2], and is prone to large error.

In conclusion, we have presented here sensitive real-time measurement of the complex refractive index of highly turbid media that is supported, for the first time, by Fresnel theory that correctly accounts for TIR from a turbid medium. We believe that, in conjunction with recent surface plasmon resonance techniques [10], our method is useful for novel biological and petroleum sensing.

We gratefully acknowledge help in LabVIEW from Mr. Lynn Johnson in the Instrumentation Laboratory at Miami University and financial support from the Petroleum Research Fund. W. R. Calhoun is now in the biomedical engineering Ph.D. program at Virginia Commonwealth University, USA.

References

1. J. Lai, Z. Li, C. Wang, and A. He, Appl. Opt. **44**, 1845 (2005).
2. S. Taylor, J. Czarnecki, and J. Masliyah, Fuel **80**, 2013 (2001).
3. K. Alexander, A. Killey, G. H. Meeten, and M. Senior, J. Chem. Soc. Faraday Trans. **77**, 361 (1981).
4. G. Meeten and A. North, Meas. Sci. Technol. **6**, 214 (1995).
5. A. Reyes-Coronado, A. Garcia-Valenzuela, C. Sanchez-Perez, R. G. Barrera, New J. Phys. **7**, 89 1 (2005).
6. I. Niskanen, J. Räty, and K.-E. Peiponen, Opt. Lett. **32**, 862 (2007).
7. M. A. Heald and J. B. Marion, *Classical Electromagnetic Radiation*, 3rd ed. (Brooks Cole, 1994)
8. M. McClimans, C. LaPlante, D. Bonner, and S. Bali, Appl. Opt. **45**, 6477 (2006).
9. A. W. Snyder and J. D. Love, Appl. Opt. **15**, 236 (1976).
10. Z. Wu, R. L. Nelson, J. W. Haus, and Q. Zhan, Opt. Lett. **33**, 551 (2008).